

Time resolved measurements of spin and carrier dynamics in InAs films

R. N. Kini,^{1,a)} K. Nontapot,¹ G. A. Khodaparast,^{1,b)} R. E. Welsch,² and L. J. Guido³

¹Department of Physics, Virginia Tech, Blacksburg, Virginia 24061, USA

²Kopin Corporation, Taunton, Massachusetts 02780, USA

³Department of Electrical and Computer Engineering, Virginia Tech, Blacksburg, Virginia 24061, USA

(Received 20 June 2007; accepted 21 January 2008; published online 27 March 2008)

We report time resolved measurements of spin and carrier relaxation in InAs films with carrier densities of 1.3×10^{16} and $1.6 \times 10^{16} \text{ cm}^{-3}$ grown on (001) and (111) GaAs, respectively. We used standard pump-probe and magneto-optical Kerr effect spectroscopy at different excitation wavelengths, power densities, and temperatures. We observed sensitivity of carrier and spin relaxation time to the photoinduced carrier density but not to the variation in temperature. We explain our results using the Elliot–Yafet picture of spin relaxation process in narrow gap semiconductors. © 2008 American Institute of Physics. [DOI: [10.1063/1.2899091](https://doi.org/10.1063/1.2899091)]

I. INTRODUCTION

Making use of electron spin in semiconductors has attracted much interest in recent years. Since the proposal by Datta and Das¹ of a spin transistor based on spin precession (which can be controlled by an external electric field via spin-orbit coupling), there has been growing interest in understanding and manipulating spin-orbit interactions in low dimensional semiconductor structures. Intense research has been focused on narrow gap semiconductors such as InAs based systems due to their expected large Rashba effect, small effective mass, large g factor, high intrinsic mobility, and large spin-orbit coupling effects. These electronic properties are vital for the emerging field of “spintronics” which attempts to combine both charge and spin degrees of freedom to improve the performance of electronic devices. A crucial factor to design the spin-sensitive devices is spin-relaxation time, which must be long enough to allow for transport and manipulation of spin-polarized carriers (for recent topical reviews see Refs. 2–5).

Recently, various measurements using differential transmission techniques to probe spin relaxation in InAs based systems have been performed. Boggess *et al.*⁶ in n -type bulk InAs with electron mobility of $2.6 \times 10^4 \text{ cm}^2/\text{V s}$ and an estimated electron density of $2 \times 10^{16} \text{ cm}^{-3}$ using polarization-resolved subpicosecond pump-probe measurements, reported spin relaxation of 19 ± 4 ps (the photoinduced carrier density was estimated to be $\sim 2 \times 10^{16} \text{ cm}^{-3}$). Direct pump-probe measurements of spin life time in intrinsic and degenerate n -InAs at 300 K reported by Murzyn *et al.*⁷ demonstrated a spin life time of 24 ± 2 ps. Hall *et al.*⁸ studied spin relaxation in (110) and (001) InAs/GaSb heterostructures using the same technique as Boggess’s earlier work but with 200 fs pulse duration (the photoinduced carrier density was estimated to be of the order of $(\sim 1-3) \times 10^{16} \text{ cm}^{-3}$). The measurements were performed at low temperature (115 K) using midinfrared (MIR) pulses ($4-4.6 \mu\text{m}$) tuned to the band gap

energy to excite only the heavy hole to conduction band transition. A spin lifetime of 18 ps in (110) superlattices was observed, much longer than the observed value of 700 fs in the (001) sample. The large enhancement has been explained by the suppression of decay associated with asymmetry in interface bonding and bulk inversion asymmetry contributions to the spin decay process in (110) superlattices. Murdin *et al.*⁹ using 100 fs laser pulses in n -InAs with doping densities between 5.2×10^{16} and $8.8 \times 10^{17} \text{ cm}^{-3}$ (for temperature ranging from 77 to 300 K), measured the spin lifetime between 5 and 50 ps. The maximum lifetime at room temperature was 24 ps for intermediate doping. Litvinenko *et al.*¹⁰ studied spin lifetime in three undoped InAs films of thicknesses 0.15, 0.27, and $1 \mu\text{m}$ and one $3\text{-}\mu\text{m}$ -thick Si-doped ($5.2 \times 10^{16} \text{ cm}^{-3}$) InAs film, for temperatures ranging from 77 to 290 K. Several spin relaxation regimes were observed and the spin lifetime was ranging from 1 ps for $0.15 \mu\text{m}$ thick layer to 20 ps for $1 \mu\text{m}$ thick layer (greater than 20 ps for the doped sample) at 77 K. The strong temperature dependence of the spin lifetime was observed only in the thickest films and a spin lifetime of shorter than 1 ps was estimated in the surface layer.

In n -type semiconductors, two relaxation processes are dominant: D’yakonov–Perel¹¹ and Elliot–Yafet¹² (EY) mechanisms. It has been theoretically predicted that for III–V bulk semiconductors, EY mechanism is dominant at very low temperatures ($T < 6$ K).¹³ However, it has been reported that this cross over can happen even at higher temperatures (~ 200 K) in low mobility ($\sim 10\,000 \text{ cm}^2/\text{V s}$) InSb quantum well samples.¹⁴ Charge accumulation at the surface is particularly strong in InAs and the electron mobility could be several orders of magnitude smaller than the bulk.¹⁵ A very short spin lifetime in the surface region of InAs was reported recently.¹⁰

The significance of the present work is the application of magneto-optical Kerr effect (MOKE) spectroscopy to probe spin relaxation in InAs compared to recent differential transmission measurements. In this work, a variation of spin relaxation (and carrier relaxation) times as a function of photoinduced carrier densities has been observed which can be explained on the basis of the EY mechanism.¹² In this

^{a)}Present address: National Renewable Energy Laboratory, Golden, CO 80401.

^{b)}Author to whom correspondence should be addressed. Electronic mail: khoda@vt.edu.

mechanism, spin relaxation time is expected to be proportional to the momentum relaxation time, which itself depends on temperature, concentration, and mobility. In our measurements, however, changing the sample temperature from room temperature (RT) to 77 K did not alter the relaxations significantly.

II. SAMPLES AND EXPERIMENTAL TECHNIQUES

In this work, the samples were InAs films with thickness of 2 μm grown on GaAs (111) and GaAs (001) substrates via metal-organic chemical vapor deposition technique (MOCVD). Both samples have a 60 nm InAs nucleation layer on the top of the GaAs. Details of this “two-step” growth method have been previously reported.¹⁶ Carrier density of the (001) film is $\sim 1.3 \times 10^{16} \text{ cm}^{-3}$ with mobilities of $\sim 20\,000$ and $10\,500 \text{ cm}^2/\text{V s}$ at 77 K and RT, respectively. For the InAs (111) film, the carrier density is $\sim 1.6 \times 10^{16} \text{ cm}^{-3}$ with mobilities of $\sim 33\,000$ and $12\,300 \text{ cm}^2/\text{V s}$ at 77 K and RT, respectively.

We used two experimental schemes to probe the dynamics, degenerate and two color pump/probe and MOKE technique. This technique has been widely used to probe spin dynamics in different material systems.^{17,18} For the degenerate scheme, the source of the pump and probe beam was a Ti-sapphire laser which generates near IR (NIR) pulses with duration of ~ 100 fs, at a repetition rate of 80 MHz, and average power of about 900 mW or a Ti:sapphire-based chirped pulse amplifier (CPA) at 800 nm with maximum average power of ~ 1 W, a pulse energy of ~ 1 mJ at 100 fs pulse duration and at repetition rate of 1 kHz. The laser beam was split using a beam splitter into a pump (90%) and probe (10%) beam. For the two-color configuration, the pump beam was MIR pulses from an optical parametric amplifier pumped by the CPA and the probe beam was NIR pulses from the CPA at 800 nm. The pump (~ 1 – 2 mW) and the probe ($\sim 5 \mu\text{W}$) beams were focused by a parabolic mirror and overlapped on the sample with a spot size of about 100–150 μm (slightly bigger for the pump).

A quarter wave plate was used to circularly polarize the pump beam to excite spin polarized carriers and a half wave plate was used to rotate the linearly polarized plane of the probe beam. As a result of selection rules for interband transitions, spin-polarized carriers can be created using circularly polarized pump beams. The MOKE signal arises from the difference between the optical coefficients of a material for left and right circularly polarized light which is proportional to the magnetization produced by the circularly polarized pump.¹⁹ Using a Wollaston prism, the reflected NIR signal was separated into *s* and *p* components which are orthogonal and have equal intensity in the equilibrium spin density state. In the presence of nonequilibrium spin polarized carriers, the MOKE signal reflects as an intensity difference between the *s* and *p* components of the reflected probe pulses. The signals were monitored using a Si balanced detector and were fed into a lock-in amplifier. A schematic representation of our experimental setup used for the time resolved MOKE experiments is shown in Fig. 1.

Under the same experimental conditions, the carrier dy-

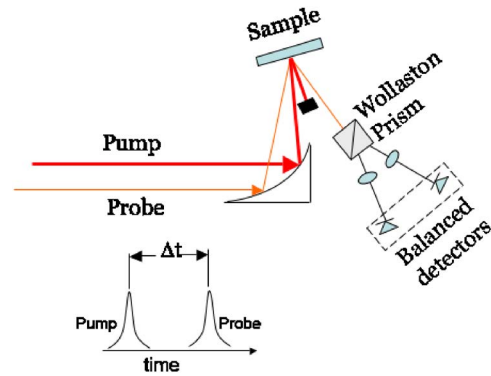


FIG. 1. (Color online) Schematic representation of the experimental setup used for time resolved MOKE experiments. The pump beam was circularly polarized and the probe beam was linearly polarized with the plane of polarization rotated 45° . A Wollaston prism was used to split the reflected probe beam into the *s* and *p* components and detected using balanced detectors.

namics were measured by probing the change of the transient reflectivity as a function of time delay between the pump and probe pulses.

III. EXPERIMENTAL RESULTS AND DISCUSSIONS

Figure 2 shows carrier and spin relaxation dynamics at RT with pump/probe fixed at 800 nm with an average power of ~ 1 mW or pump fluence of $5 \text{ mJ}/\text{cm}^2$ which resulted in a photoexcited carrier density of $\sim 10^{19} \text{ cm}^{-3}$. In this context, the relaxation time is referred to as the time the signal at positive time delay takes to approximately reach the value at negative time delays. The differential reflectivity as a function of time delay is shown in Fig. 2(a). The carrier relaxations in both InAs samples exhibit relaxation times of ~ 5 ps. Under the same experimental conditions as in Fig. 2(a), the MOKE signals for different circular polarizations of the pump are shown in Fig. 2(b). The spin relaxation times lasted for ~ 2 ps which is significantly faster than the relax-

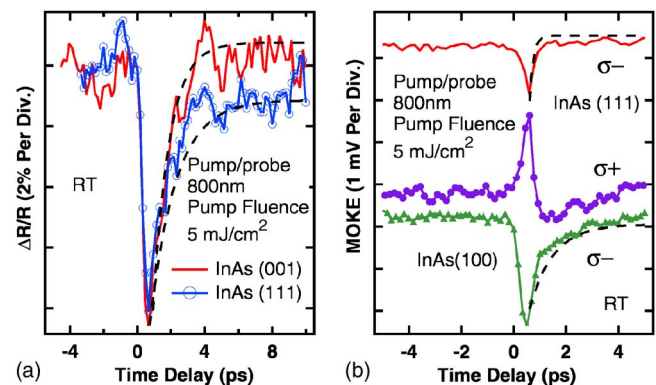


FIG. 2. (Color online) Time resolved measurements at RT with pump/probe wavelengths fixed at 800 nm. The laser fluence was about $5 \text{ mJ}/\text{cm}^2$ which resulted in a photoinduced carrier density of $\sim 10^{19} \text{ cm}^{-3}$. (a) Differential reflectivity of InAs grown on (100) and (111) GaAs as a function of time delay between pump and probe, which demonstrates carrier relaxation times of ~ 5 ps. (b) MOKE measurements on both samples at different circular polarization of the pump, demonstrates spin relaxation of ~ 2 ps. For simplicity, the measurement for only one circular polarization of the pump is shown for the InAs(111) sample. The dashed lines represent exponential fits to the data and for clarity are slightly shifted.

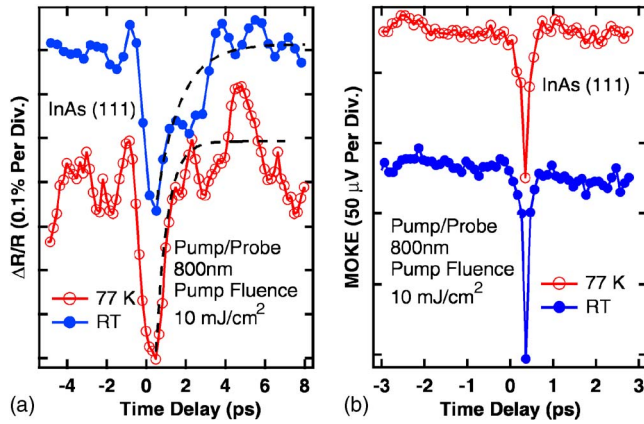


FIG. 3. (Color online) Similar measurements as in Fig. 2 with a slightly higher laser fluence of about 10 mJ/cm^2 on InAs (111) at RT and 77 K. (a) The differential reflectivity does not show a significant change compared to the measurements in Fig. 2(a). (b) MOKE measurements on the sample show spin relaxation times which are about a factor of two faster compared to the pumping regime shown in Fig. 2(b). In addition, the temperature dependence of the relaxations from RT to 77 K is not significant. The dashed lines represent exponential fits to the data and for clarity are slightly shifted.

ation of photoinduced carriers. As shown in Fig. 3 for InAs (111), by increasing the laser fluence by a factor of two compared to the measurements in Fig. 2, the carrier relaxation remained almost the same but a spin relaxation of $\sim 1 \text{ ps}$ was measured. In addition, the temperature dependence of the relaxations was not significant.

The measurements presented in the Figs. 2 and 3 were performed in a degenerate pump/probe scheme where effects such as band filling could be important and affect the dynamic. As shown in Fig. 4, we also used a two-color scheme at RT and 77 K with the pump and probe fixed at $2 \mu\text{m}$ and 800 nm, respectively. The laser fluence and, therefore, the photoinduced carrier density is the same as the measurements presented in Fig. 2. In this case, the differential reflectivity and MOKE measurement demonstrate carrier and spin relaxation times similar to those observed in Fig. 2. We attribute the decrease in the observed differential reflectivity to free carrier Drude absorption by the photoinduced carriers.

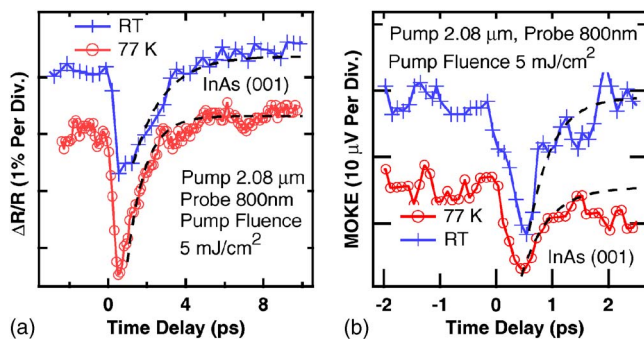


FIG. 4. (Color online) Time resolved measurements of InAs grown on (100) GaAs at RT and 77 K with pump/probe wavelengths fixed at $2 \mu\text{m}$ and 800 nm, respectively. The laser fluence was about 5 mJ/cm^2 which resulted in a photoinduced carrier density of $\sim 10^{19} \text{ cm}^{-3}$ (a) Differential reflectivity as a function of time delay between pump and probe which demonstrates carrier relaxation times similar to the observed in Fig. 2(a). (b) MOKE measurements similar to the case shown in Fig. 2(b). The dashed lines represent exponential fits to the data and for clarity are slightly shifted.

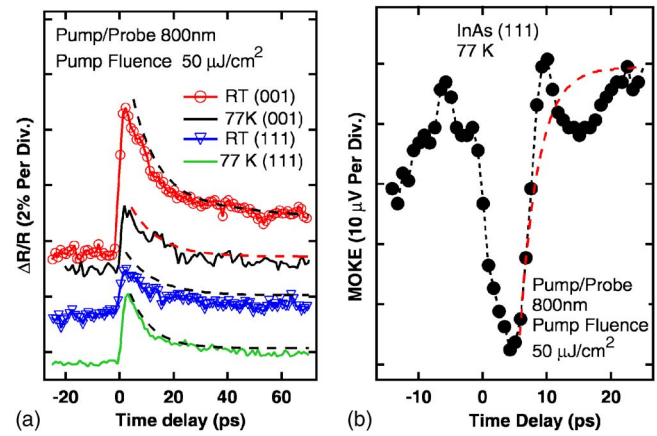


FIG. 5. (Color online) Time resolved measurements with pump/probe wavelengths fixed at 800 nm with a laser fluence of about $50 \mu\text{J/cm}^2$ which resulted in a photoinduced carrier density of $\sim 10^{17} \text{ cm}^{-3}$. (a) Differential reflectivity of InAs grown on (100) and (111) GaAs as a function of time delay between pump and probe at RT and 77 K. A biexponential function was used to fit the data (dashed lines). The faster component of the relaxation was greater than 20 ps. (b) An example of MOKE measurements (at 77 K) of the InAs (111) for one circular polarization of the pump is plotted. The spin relaxation is faster than the carrier relaxation but a significant enhancement compared to Figs. 2(b) and 3(b) has been observed. The dashed line represents exponential fit to the data and for clarity is shifted slightly.

In order to probe the relaxations in much lower excitation regime, the laser fluence was reduced from 5 mJ/cm^2 to $50 \mu\text{J/cm}^2$ (using the 80 MHz system). As shown in Fig. 5, an enhancement in carrier and spin relaxation were observed compared to the high laser fluence regimes with no strong temperature dependence. In this regime, where the pump/probe excitation wavelengths are the same as Figs. 2 and 3 (but the laser fluence is much smaller) the differential reflectivity is positive. In contrast to free carrier absorption, the mechanism of band filling results in a positive change in differential reflectivity. In the case of other mechanisms such as band gap renormalization, the change in refractive index should be largest near the band edge and decreases rapidly with increasing probe photon energy. Therefore, this effect is not significant at our probe wavelength, which is far away from the band edge.

IV. SUMMARY

In summary, we studied carrier/spin dynamics of two InAs samples grown on (001) and (111) GaAs by MOCVD. We employed two time resolved schemes (degenerate and nondegenerate) with different laser fluences in the reflectivity geometry to probe the relaxation dynamics. The observations in these samples demonstrated the sensitivity of the relaxations to the density of photoinduced carriers. Unlike the earlier reported measurements on thick InAs films, no strong variation in the dynamics was observed from RT to 77 K in these studies. In the low laser fluence regime, our spin relaxation times are in the range of earlier observations in InAs (Refs. 6, 7, 9, and 10) with a similar photoinduced carrier density. In the high laser fluence regime, our observed fast spin relaxation (1–2 ps) is comparable to an earlier measurement on $0.15 \mu\text{m}$ thick film¹⁰ where the contribution

from the inversion layer is considered to dominate. At higher laser fluences with larger photoinduced carrier density, a faster momentum scattering time is expected. In the EY picture, the spin relaxation time is linearly proportional to momentum scattering time; therefore, our observation of shorter spin relaxation time at higher fluence suggests that EY mechanism is dominating the spin relaxation process in the temperature range of our measurements.

ACKNOWLEDGMENTS

This work has been supported by NSF Grant No. DMR-0507866, AFOSR Young Investigator Program 06NE231, Jeffress Trust Fund J748, Advance-VT, and the NSF-STTR Program (Award No. 0638227).

¹S. Datta and B. Das, *Appl. Phys. Lett.* **56**, 665 (1990).

²D. D. Awschalom and M. E. Flatté, *Nat. Phys.* **3**, 153 (2007).

³I. Zutic, J. Fabian, and S. Das Sarma, *Rev. Mod. Phys.* **76**, 323 (2004).

⁴R. H. Silsbee, *J. Phys.: Condens. Matter* **16**, R179 (2004).

⁵W. Zawadzki and P. Pfeffer, *Semicond. Sci. Technol.* **19**, R1 (2004).

⁶T. F. Boggess, J. T. Olesberg, C. Yu, M. E. Flatté, and W. H. Lau, *Appl. Phys. Lett.* **77**, 1333 (2000).

⁷P. Murzyn, C. R. Pidgeon, P. J. Phillips, M. Merrick, K. L. Litvinenko, J. Allam, B. N. Murdin, T. Ashley, J. H. Jefferson, and L. F. Cohen, *Appl.*

Phys. Lett. **83**, 5220 (2003).

⁸K. C. Hall, K. Gündogdu, E. Altunkaya, W. H. Lau, M. E. Flatté, T. F. Boggess, J. J. Zinck, W. B. Barvosa-Carter, and S. L. Skeith, *Phys. Rev. B* **68**, 115311 (2003).

⁹B. N. Murdin, K. Litvinenko, J. Allam, C. R. Pidgeon, M. Bird, K. Morrison, T. Zhang, S. K. Clowes, W. R. Branford, J. Harris, and L. F. Cohen, *Phys. Rev. B* **72**, 085346 (2005).

¹⁰K. L. Litvinenko, B. N. Murdin, J. Allam, T. Zhang, J. J. Harris, L. F. Cohen, D. A. Eustace, and D. W. McComb, *Phys. Rev. B* **74**, 075331 (2006).

¹¹M. I. D'yakonov and V. I. Perel, *Sov. Phys. Solid State* **13**, 3023 (1972).

¹²R. J. Elliot, *Phys. Rev.* **96**, 266 (1954); Y. Yafet, *Solid State Physics*, edited by F. Seitz and D. Turnbull (Academic, New York, 1963), Vol. 14.

¹³P. H. Song and K. W. Kim, *Phys. Rev. B* **66**, 035207 (2002).

¹⁴K. L. Litvinenko, B. N. Murdin, J. Allam, C. R. Pidgeon, M. Bird, K. Morris, W. Branford, S. K. Clowes, L. F. Cohen, T. Ashley, and L. Buckle, *New J. Phys.* **8**, 491 (2006).

¹⁵H. A. Washburn, J. R. Sites, and H. H. Wiender, *J. Appl. Phys.* **50**, 4872 (1979).

¹⁶R. E. Welser and L. J. Guido, *Appl. Phys. Lett.* **68**, 912 (1996).

¹⁷D. D. Awschalom, D. Loss, and N. Samarth, *Semiconductor Spintronics and Quantum Computation*, edited by D. D. Awschalom, D. Loss, and N. Samarth (Springer, Berlin, 2002).

¹⁸J. Wang, C. Sun, Y. Hashimoto, J. Kono, G. A. Khodaparast, L. Cywinski, L. J. Sham, G. D. Sanders, C. J. Stanton, and H. Munekata, *J. Phys.: Condens. Matter* **18**, R501 (2006).

¹⁹A. K. Zvezdin and V. A. Kotov, *Modern Magneto-optics and Magneto-optical Materials* (IoP, Bristol, 1997).